

# Evaluation of the dependence of the sensible heat flux trend on elevation over the Tibetan Plateau in CMIP5 models

Lihua Zhu<sup>1,2</sup> | Gang Huang<sup>3,4,5</sup>  | Guangzhou Fan<sup>1</sup> | Xia Qü<sup>6</sup> |  
Zhibiao Wang<sup>6</sup> | Wei Hua<sup>1</sup> | Xin Lai<sup>1</sup>

<sup>1</sup>School of Atmospheric Sciences/Plateau Atmosphere and Environment Key Laboratory of Sichuan Province/Joint Laboratory of Climate and Environment Change, Chengdu University of Information Technology, Chengdu, China

<sup>2</sup>Heavy Rain and Drought-Flood Disasters in Plateau and Basin Key Laboratory of Sichuan Province, Chengdu, China

<sup>3</sup>State Key Laboratory of Numerical Modeling for Atmospheric Sciences and Geophysical Fluid Dynamics, Institute of Atmospheric Physics, Chinese Academy of Sciences, Beijing, China

<sup>4</sup>Laboratory for Regional Oceanography and Numerical Modeling, Qingdao National Laboratory for Marine Science and Technology, Qingdao, China

<sup>5</sup>University of Chinese Academy of Sciences, Beijing, China

<sup>6</sup>Center for Monsoon System Research, Institute of Atmospheric Physics, Chinese Academy of Sciences, Beijing, China

## Correspondence

Gang Huang, State Key Laboratory of Numerical Modeling for Atmospheric Sciences and Geophysical Fluid Dynamics, Institute of Atmospheric Physics, Chinese Academy of Sciences, Beijing 100029, China.  
Email: hg@mail.iap.ac.cn

## Funding information

Sichuan Science and Technology Program, Grant/Award Numbers: 2019YJ0359, 2019YJ0362; the Heavy Rain and Drought-Flood Disasters in Plateau and Basin Key Laboratory of Sichuan Province, Grant/Award Number: SZKT201906; Foundation for Innovative Research Groups of the National Natural Science Foundation of China, Innovative Research Group Project of the National Natural Science Foundation of China, Grant/Award Numbers: 41721004, 41831175, 41975130, 42075019, 91937302; the Sichuan Provincial Department of Education Project of China, Grant/Award Number: 15ZB0170; the Strategic Priority Research Program of the Chinese Academy of Sciences, Grant/Award Number: XDA20060501

## Abstract

We evaluated the dependence of the sensible heat flux trend over the Tibetan Plateau on elevation by comparing the 29 climate models in the Coupled Model Intercomparison Project Phase 5 (CMIP5) with ground observations in the time period 1980–2005. The sensible heat flux trend over the Tibetan Plateau shows an elevation-dependent variation in both the observations and reanalysis datasets, with a larger negative trend at higher altitudes. Most of the models analysed in this study performed poorly in simulating the linear trend of the sensible heat flux, although two models (HadGEM2-CC and HadGEM2-ES) reasonably captured the elevation range and seasons with a prominent decreasing trend in the sensible heat flux over the Tibetan Plateau. These two models possess good skills in depicting both the sensible heat flux trend and the terrain of the plateau in every 1,000 m wide altitudinal band. The coherence of the elevation-dependent variation in the sensible heat flux trend between the observations and models is therefore not fortuitous. The sensible heat flux trend in most models of CMIP5 is sensitive to variations in the surface wind speed and the difference in temperature between the ground surface and the air, although these two factors show large biases deviating from the reanalysis product in almost all models in this study. In the HadGEM2-CC and HadGEM2-ES models, which showed a good performance in capturing the elevation-dependent sensible heat flux trend, the leaf area index was shown to be the predominant factor affecting the variation in the sensible heat flux trend with elevation. That maybe link with the dynamic vegetation scheme in these two models.

**KEYWORDS**

altitude dependence, CMIP5, surface sensible heat flux trend, Tibetan Plateau

**1 | INTRODUCTION**

The Tibetan Plateau—with a zonal length of 2,800 km, a meridional width of 300–1,500 km and an average altitude >4,000 m—is the largest high-altitude plateau in the world. The thermal and mechanical effects of forcing by the Tibetan Plateau have a crucial role in the regional and global climate (e.g., Yeh *et al.*, 1957; Yeh and Gao, 1979; Yanai *et al.*, 1992; Ye and Wu, 1998; Chakraborty *et al.*, 2002; Duan and Wu, 2005; Chakraborty *et al.*, 2006; Wu *et al.*, 2007; Boos and Kuang, 2010; Duan *et al.*, 2012; Wu *et al.*, 2012a; Yao *et al.*, 2012; Wu *et al.*, 2014). The Tibetan Plateau acts as an immense, intense and elevated heat source and its surface layers are an important store of sensible heat (e.g., Yeh *et al.*, 1957; Yeh and Gao, 1979; Duan and Wu, 2008; Yang *et al.*, 2011; Wu *et al.*, 2014). The Tibetan Plateau uses sensible heat to drive the movement of air masses and water vapor in the low-level atmosphere, triggering convective precipitation and the release of latent heat (e.g., Wan and Wu, 2007; Wu *et al.*, 2007; Wan *et al.*, 2009; Duan *et al.*, 2011; Liu *et al.*, 2012; Wu *et al.*, 2012b; Duan *et al.*, 2013; Wang *et al.*, 2014; Wu *et al.*, 2014; Wu *et al.*, 2016). This process is described as sensible heating atmosphere pumping (Wu *et al.*, 1997; Wu *et al.*, 2007; Wu *et al.*, 2014). The sensible heat over the Tibetan Plateau exerts a great influence on the onset and maintenance of the Asian summer monsoon (e.g., Yeh *et al.*, 1957; Flohn, 1957, 1960; Yanai *et al.*, 1992; Wu *et al.*, 2012a, 2012b, 2012c; Liu *et al.*, 2013; Wu *et al.*, 2014) and the evolution of atmospheric circulation and climate anomalies via the dispersion of Rossby waves (Wu *et al.*, 2012a; Wang *et al.*, 2014; Wu *et al.*, 2014; Wu *et al.*, 2016).

There is growing evidence that the sensible heat flux over the Tibetan Plateau has decreased since the 1980s (Duan and Wu, 2008; Duan *et al.*, 2011; Duan *et al.*, 2013; Zhu *et al.*, 2019). This weakening trend shows an elevation-dependent variation in observational data (Zhu *et al.*, 2019). The sensible heat flux over the Tibetan Plateau and its pivotal role in climate change are directly related to the high altitude of this region. The mechanism of elevated heating has been reported previously (Yeh and Gao, 1979; Molnar and Emanuel, 1999; Wu *et al.*, 2014; Hu and Boos, 2017a, 2017b), but studies of the dependence of the sensible heat flux on elevation are still limited.

Studies of the variation in sensible heat flux with altitude will contribute to reducing the current uncertainties about the climate in remote, high-elevation regions and

ensure that the variations related to the sensible heat flux (e.g., the exchange of heat and moisture between the Earth's surface and the atmosphere, the redistribution of energy, the exchange of momentum, the evolution of atmospheric circulation, and anomalies in the regional and global climate) are adequately monitored and accounted for.

The Tibetan Plateau, often referred to as the water tower of Asia, is the source of many important Asian rivers (Immerzeel *et al.*, 2010; Yao *et al.*, 2012) and the major source of water for large populations in lower elevation regions (Viviroli *et al.*, 2007). Precipitation on the Tibetan Plateau has a remarkable influence on the water level in lakes, the runoff from rivers, and droughts and floods in downstream regions. The sensible heat over the Tibetan Plateau is a crucial factor in precipitation on the plateau. The social and economic impacts arising from variations in precipitation associated with the sensible heat flux over the Tibetan Plateau could therefore be large and justify further research.

Zhu *et al.* (2019) reported that a larger negative trend in the sensible heat flux is seen at higher altitudes. We aimed to determine whether this dependence of the sensible heat flux trend on elevation is also present in reanalysis datasets and how well the models in the Coupled Model Intercomparison Project Phase 5 (CMIP5) simulate the variation of the sensible heat flux trend with altitude. As a result of the scarcity of observations at high elevations, evidence for the dependence of the sensible heat flux trend on elevation will need to be obtained from other datasets (e.g., atmospheric reanalysis and model simulations) to reduce the current uncertainties and to confirm the variations in high-altitude regions. It is particularly important to evaluate and improve the models under the realistic assumption that the in situ climate observing network on the Earth's surface is limited by geographical constraints in many high-altitude areas. This study therefore attempted to identify the dependence of the variation in the sensible heat flux trend on elevation in reanalysis datasets and to quantify the performance of models in simulating this dependency, which may be an important aspect in model verification.

The structure of this article is as follows. A brief description of the datasets and applied methodology is presented in Section 2. Using reanalysis datasets, the dependence of the sensible heat flux trend over the Tibetan Plateau on elevation is reconfirmed in Section 3.

Section 4 evaluates the performance of the CIMP5 climate models in simulating the dependence of the sensible heat flux trend over the Tibetan Plateau on elevation and to tries to identify the cause of this trend. We briefly outline our discussion and conclusions in Section 5.

## 2 | DATA AND METHODOLOGY

### 2.1 | Data

The data were obtained from the following sources.

1. Regular surface observations from 140 meteorological stations on the Tibetan Plateau operated by the China Meteorological Administration. These include measurements made four times each day of the ground surface temperature at 0 cm depth ( $T_s$ ), the surface air temperature ( $T_a$ ) and the wind speed at 10 m above the surface ( $V_0$ ). Missing values occur mostly before 1980s; hence, the observations after 1980 are utilized in this study to ensure a reliable outcome. The missing values of variables in the observations account for less than 0.5% of the total records during the studied period, accordingly the quality of the observational data is reasonably good. The method of processing missing values in the observational data is the same as applied in the study by Duan and Wu (2008). Figure 1 shows the elevations and locations of the 140 stations. Of these stations, 82 (58.6%) are above 2,000 m, 48 (34.3%) are above 3,000 m, and 16 (11.4%) are above 4,000 m.
2. To overcome the limitations resulting from the sparseness of in situ ground measurements in under-sampled high-altitude regions, the reanalysis datasets were used to identify and quantify the dependence of the sensible heat flux trend on elevation. Monthly mean of

sensible heat flux from the National Centres for Environmental Prediction/National Center for Atmospheric Research (NCEP/NCAR) Reanalysis 1 dataset (Kalnay *et al.*, 1996, [www.esrl.noaa.gov/psd/data/gridded/data.ncep.reanalysis.html](http://www.esrl.noaa.gov/psd/data/gridded/data.ncep.reanalysis.html)), the NCEP/Department of Energy (NCEP/DOE) Reanalysis 2 dataset (Kanamitsu *et al.*, 2002, [www.esrl.noaa.gov/psd/data/gridded/data.ncep.reanalysis2.html](http://www.esrl.noaa.gov/psd/data/gridded/data.ncep.reanalysis2.html)), the Japanese 25-year Reanalysis (JRA-25) dataset (Onogi *et al.*, 2007, <https://climatedataguide.ucar.edu/climate-data/jra-25>), and the European Centre for Medium-Range Weather Forecasts Reanalysis Interim (ERA-Interim) dataset (Dee *et al.*, 2011; <http://apps.ecmwf.int/datasets>) were analysed simultaneously in this study. Other data sets include monthly surface 2 m air temperature, soil temperature at the depth below land surface, surface 10 m zonal wind and surface 10 m meridional wind from JRA-25. The NCEP/NCAR and NCEP/DOE reanalysis datasets are provided on a Gaussian grid with  $192 \times 94$  data points. The JRA-25 reanalysis is provided on a  $320 \times 160$  regular Gaussian grid (east–west: 125.069 km just north and south of the Equator to 1.874 km near the poles). And the ERA-Interim dataset is resolved on a  $1^\circ \times 1^\circ$  grid.

3. Monthly outputs from historical climate experiments in 29 CMIP5 climate models are analysed and compared (Table 1; [www.ipcc-data.org/sim/gcm\\_monthly/AR5/Reference-Archive.html](http://www.ipcc-data.org/sim/gcm_monthly/AR5/Reference-Archive.html)), including surface sensible heat flux, near-surface air temperature, surface temperature, near-surface wind speed, leaf area index, and surface snow amount.

The boundary of the Tibetan Plateau for each reanalysis dataset and model in this study was defined as the domain ( $25^\circ$ – $40^\circ$ N,  $70^\circ$ – $110^\circ$ E) and the grid points below 1,000 m were discarded. The temporal periods of the data used in this study are all from January 1980 to December 2005.

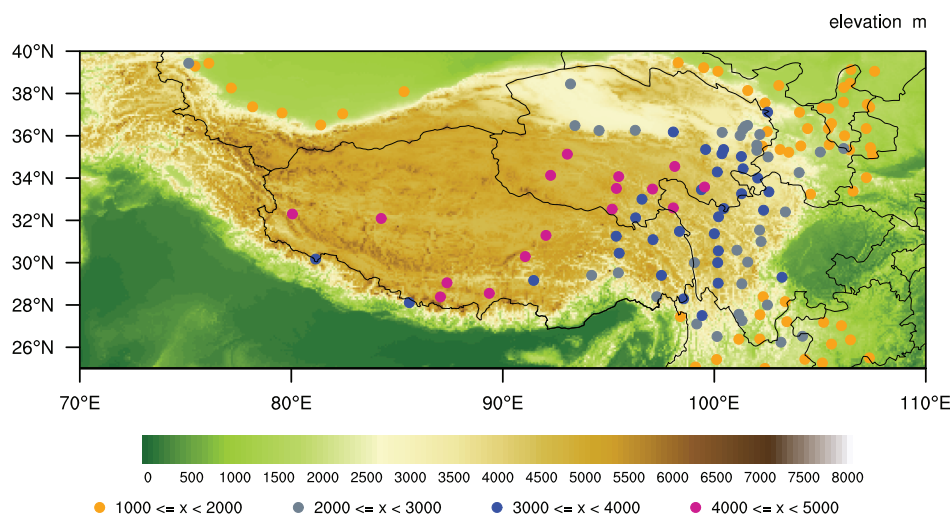


**FIGURE 1** Elevations and locations of meteorological stations above 1,000 m on the Tibetan Plateau

**TABLE 1** Basic information for the 29 CMIP5 climate models

| Model name     | Modelling centre(or group)                                                                                                                                                       | Atmospheric resolution (long. × lat.) |
|----------------|----------------------------------------------------------------------------------------------------------------------------------------------------------------------------------|---------------------------------------|
| ACCESS1.0      | Commonwealth Scientific and Industrial Research Organization, Australia and Bureau of Meteorology, Australia                                                                     | 192 × 145                             |
| ACCESS1.3      | Commonwealth Scientific and Industrial Research Organization, Australia and Bureau of Meteorology, Australia                                                                     | 192 × 145                             |
| CanESM2        | Canadian Centre for Climate Modelling and Analysis                                                                                                                               | 128 × 64                              |
| CMCC-CESM      | Centro euro-Mediterraneo sui Cambiamenti Climatici                                                                                                                               | 96 × 48                               |
| CMCC-CM        | Centro euro-Mediterraneo sui Cambiamenti Climatici                                                                                                                               | 480 × 240                             |
| CMCC-CMS       | Centro euro-Mediterraneo sui Cambiamenti Climatici                                                                                                                               | 192 × 96                              |
| CNRM-CM5       | Centre National de Recherches <i>Météorologique</i> /Centre Européen de Recherche et de Formation Avancées en Calcul Scientifique                                                | 256 × 128                             |
| CNRM-CM5-2     | Centre National de Recherches <i>Météorologique</i> /Centre Européen de Recherche et de Formation Avancées en Calcul Scientifique                                                | 256 × 128                             |
| CSIRO-Mk3.6.0  | Commonwealth Scientific and Industrial Research Organization in collaboration with the Queensland Climate Change Centre of Excellence                                            | 192 × 96                              |
| GFDL-CM2.1     | National Oceanic and Atmospheric Administration Geophysical Fluid Dynamics Laboratory                                                                                            | 144 × 90                              |
| GFDL-CM3       | National Oceanic and Atmospheric Administration Geophysical Fluid Dynamics Laboratory                                                                                            | 144 × 90                              |
| GFDL-ESM2G     | National Oceanic and Atmospheric Administration Geophysical Fluid Dynamics Laboratory                                                                                            | 144 × 90                              |
| GISS-E2-H      | National Aeronautics and Space Administration Goddard Institute for Space Studies                                                                                                | 144 × 90                              |
| GISS-E2-R      | National Aeronautics and Space Administration Goddard Institute for Space Studies                                                                                                | 144 × 90                              |
| HadCM3         | UK Meteorological Office Hadley Centre (additional HadGEM2-ES realizations contributed by Instituto Nacional de Pesquisas Espaciais)                                             | 96 × 73                               |
| HadGEM2-CC     | UK Meteorological Office Hadley Centre (additional HadGEM2-ES realizations contributed by Instituto Nacional de Pesquisas Espaciais)                                             | 192 × 145                             |
| HadGEM2-ES     | UK Meteorological Office Hadley Centre (additional HadGEM2-ES realizations contributed by Instituto Nacional de Pesquisas Espaciais)                                             | 192 × 145                             |
| IPSL-CM5A-LR   | Institute Pierre-Simon Laplace                                                                                                                                                   | 96 × 96                               |
| IPSL-CM5A-MR   | Institute Pierre-Simon Laplace                                                                                                                                                   | 144 × 143                             |
| IPSL-CM5B-LR   | Institute Pierre-Simon Laplace                                                                                                                                                   | 96 × 96                               |
| MIROC-ESM-CHEM | Japan Agency for Marine-Earth Science and Technology, Atmosphere and Ocean Research Institute (The University of Tokyo) and the National Institute for Environmental Studies     | 128 × 64                              |
| MIROC-ESM      | Japan Agency for Marine-Earth Science and Technology, Atmosphere and Ocean Research Institute (The University of Tokyo) and the National Institute for Environmental Studies     | 128 × 64                              |
| MIROC4h        | Atmosphere and Ocean Research Institute (The University of Tokyo), the National Institute for Environmental Studies and the Japan Agency for Marine-Earth Science and Technology | 640 × 320                             |

**TABLE 1** (Continued)

| Model name | Modelling centre(or group)                                                                                                                                                       | Atmospheric resolution (long. × lat.) |
|------------|----------------------------------------------------------------------------------------------------------------------------------------------------------------------------------|---------------------------------------|
| MIROC5     | Atmosphere and Ocean Research Institute (The University of Tokyo), the National Institute for Environmental Studies and the Japan Agency for Marine-Earth Science and Technology | 256 × 128                             |
| MPI-ESM-LR | Max Planck Institute for Meteorology                                                                                                                                             | 192 × 96                              |
| MPI-ESM-MR | Max Planck Institute for Meteorology                                                                                                                                             | 192 × 96                              |
| MPI-ESM-P  | Max Planck Institute for Meteorology                                                                                                                                             | 192 × 96                              |
| MRI-CGCM3  | Meteorological Research Institute                                                                                                                                                | 320 × 160                             |
| MRI-ESM1   | Meteorological Research Institute                                                                                                                                                | 320 × 160                             |

## 2.2 | Methods

The method used to calculate the sensible heat flux from the observations is the same as applied in previous research related to the Tibetan Plateau (e.g., Yeh and Gao, 1979; Chen *et al.*, 1985; Li *et al.*, 2001; Duan and Wu, 2008; Duan *et al.*, 2011, 2013; Cui *et al.*, 2015; Zhu *et al.*, 2017; Zhu *et al.*, 2019):

$$SH = C_p \rho_a C_{DH} V_0 (T_s - T_a) \quad (1)$$

where SH is the sensible heat flux,  $C_p = 1005 \text{ J} \cdot \text{kg}^{-1} \cdot \text{K}^{-1}$  is the specific heat of dry air at constant pressure,  $\rho_a$  is the density of air,  $C_{DH}$  is the drag coefficient for heat,  $V_0$  is the mean surface wind speed measured 10 m above the ground and  $(T_s - T_a)$  is the difference in temperature between the ground and the air. The changes in  $\rho_a$  and  $C_{DH}$  should be subtle during the study period (Zhu *et al.*, 2017) and their influence on the variation in the sensible heat flux is negligible, although they vary from location to location. Therefore, based on previous studies, we assume  $C_{DH} = 4 \times 10^{-3}$  for the region east of  $85^\circ\text{E}$  and  $C_{DH} = 4.75 \times 10^{-3}$  for the region west of  $85^\circ\text{E}$  (e.g., Li and Yanai, 1996; Duan and Wu, 2008; Duan *et al.*, 2011, 2013; Zhu *et al.*, 2017, 2019) and  $\rho_a = 0.8 \text{ kg} \cdot \text{m}^{-3}$  (e.g., Yeh and Gao, 1979; Duan and Wu, 2008; Duan *et al.*, 2011, 2013; Zhu *et al.*, 2019). The climatology of the seasonally averaged sensible heat flux over the Tibetan Plateau is calculated based on the 6-h sensible heat flux obtained using this equation. Simple linear regression is used to calculate the trend of the sensible heat flux based on the seasonal averages of each year for observations, reanalysis products and models. Moreover, correlation and regression analyses are used in this study to find possible linear relationships between two variables. The statistical significance is based on the Student's *t* test.

## 3 | ELEVATION-DEPENDENT VARIATION OF THE SENSIBLE HEAT FLUX TREND IN THE REANALYSIS DATASETS

To display the elevation-dependent variation of the sensible heat flux trend more intuitively, we arranged the sensible heat flux trend in a sequence ordered from low to high elevation. The sensible heat flux trend in the observations shows that most areas of the Tibetan Plateau have experienced a statistically significant decreasing trend in the sensible heat flux during the time period 1980–2005, especially above 2000 m elevation in spring and summer. The higher the altitude, the larger the negative trend. The sensible heat flux trend in the four reanalysis datasets shows an analogous elevation-dependent variation to the observations (Figure 2, left-hand panels), characterized by a negative correlation between the sensible heat flux trend and elevation for most seasons in all reanalysis datasets, although the correlation is not significant for the NCEP1 product in all seasons and for the ERA product in winter and spring (Figure 2, right-hand panels). This further confirms previously published results (Zhu *et al.*, 2019). The sensible heat flux trend over the Tibetan Plateau in the JRA-25 reanalysis dataset is the closest to the observations. We then investigated whether the elevation-dependent variation in sensible heat flux trend emerges in the CMIP5 models.

## 4 | EVALUATION OF ELEVATION-DEPENDENT SENSIBLE HEAT FLUX TREND IN THE CMIP5 MODELS

### 4.1 | Evaluation

Figure 3 compares the sensible heat flux trend over the Tibetan Plateau in the 29 climate models of CMIP5 with the ground observations. Most of the models in Figure 3

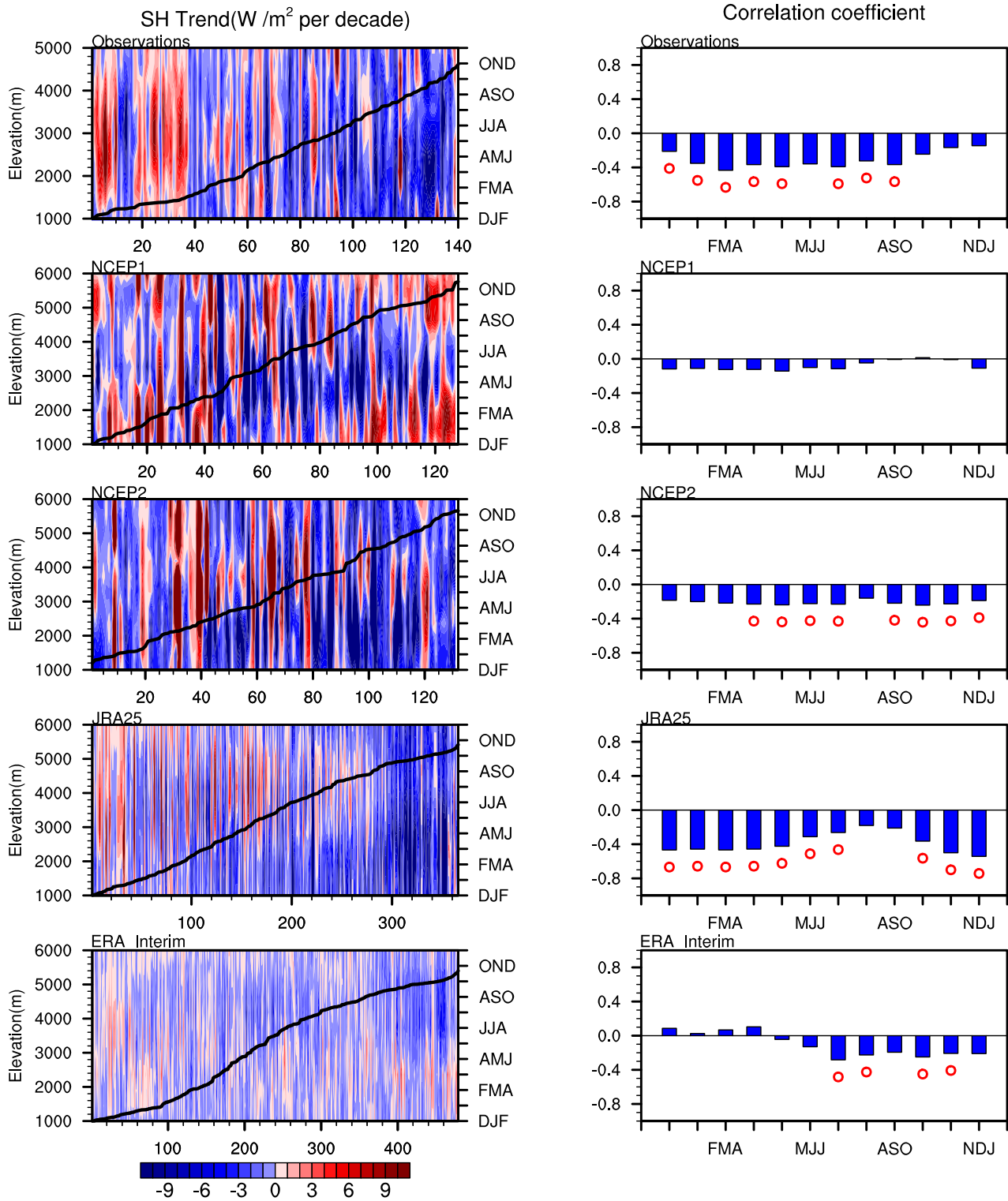


**FIGURE 2** Elevation-dependent variation of the sensible heat flux trend in the observations and four reanalysis datasets during the time period 1980–2005 (left-hand column). The stations are ordered from low to high elevation and the sequence numbers are shown on the abscissas. The black curve shows the elevation. The right-hand panels show the correlation coefficients between the sensible heat flux trends and elevations for the observations and four reanalysis datasets. The red open circles represent values exceeding the 90% significance level

show a large bias in the linear trend of the sensible heat flux, with a weaker or even opposite tendency at high altitude or over the whole plateau. However, several

models are able to capture the decreasing trend in sensible heat flux, especially at high altitude. The HadGEM2-CC and HadGEM2-ES models show good skill

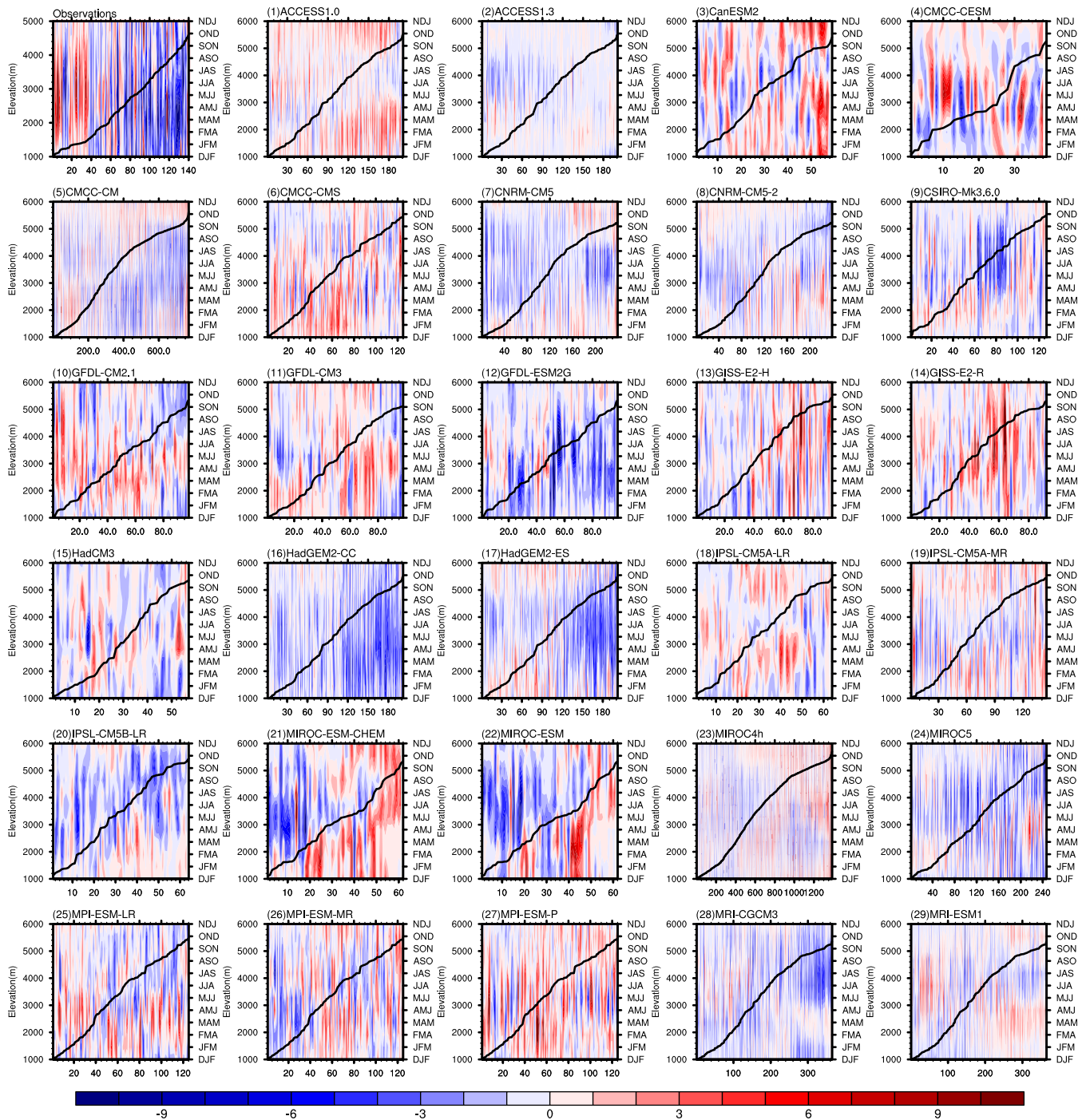


**FIGURE 3** Elevation-dependent variation of the sensible heat flux trend in the observations and the 29 climate models in CMIP5 over the Tibetan Plateau during the time period 1980–2005. The stations are ordered from low to high elevation and the sequence numbers are shown on the abscissas. The black curve shows the elevation. Units:  $W\ m^{-2}\ (10\ yr)^{-1}$

in depicting the elevation-dependent sensible heat flux trend, performing reasonably well in simulating the remarkable range of elevation and seasons of the weakening trend in sensible heat over the Tibetan Plateau.

To evaluate more intuitively the ability of the models to simulate the altitude-dependent sensible heat flux

trend, the correlation coefficients between the sensible heat flux trends and elevations in every season were calculated (Figure 4). Compared with the observations, the HadGEM2-CC and HadGEM2-ES models performed well overall in capturing the main features for the variation in the sensible heat flux trend with altitude, which is

characterized by the significantly negative correlation of the sensible heat flux trend with elevation in most seasons. This is basically consistent with the observations, except for a slight difference in significance (Figure 4).

We next investigated whether the CMIP5 models, especially the HadGEM2-CC and HadGEM2-ES models, performed consistently in simulating the variation of sensible heat flux trend from lower to higher altitudes. Considering that the most significant sensible heat flux trend and its notable dependence on altitude is in spring, we take spring as an example to further discuss the performance of the 29 CMIP5 models at different altitudes. To overcome the limitations arising from the sparseness of in situ stations over the western Tibetan Plateau, we used the JRA25 reanalysis dataset as the reference observations in the following analysis. As shown earlier, the JRA25 dataset shows the highest consistency with the meteorological observations among the four reanalysis datasets. To make a more direct comparison with the reference observations, all the model data were interpolated onto the JRA25 grid using spatial bilinear interpolation. To unify the number of grid points above a certain height among the different models, the altitudinal ranges in the following figures refer to the elevation in the JRA25 dataset.

Figure 5 show the linear variation of the sensible heat flux in the reanalysis product and the 29 climate models in CMIP5 over the Tibetan Plateau above 1,000 m. The higher the altitude, the poorer the simulation skill shown by most of the models. Among the 29 CMIP5 models, the HadGEM2-CC and HadGEM2-ES models best simulated the spatial distribution of the sensible heat flux trend from low to high altitudes. At all altitude levels, the spatial correlation coefficients for the sensible heat flux trend between the reanalysis product and the two models were all  $>0.5$ , which exceeds the 99% confidence level.

To quantitatively analyse the simulation of the 29 CMIP5 models, the correlation coefficients of the sensible heat flux trend between the reanalysis product and models for every successive 201 stations ordered from low to high elevations are shown in Figure 6. As the first step of calculating the correlation coefficients, we arranged the sensible heat flux trend in both models and reanalysis product into a sequence according to the low-to-high altitudinal order of every grid cell in the reanalysis product. The correlation coefficient is calculated, based on the sensible heat flux trend of the first successive 201 samples in reanalysis product and models, and then the sample selection glides along the altitude with the sample size unchanged. The values were multiplied by either 1 or  $-1$  depending on whether the regional mean sensible heat flux trend in the reanalysis product and each CMIP5 model had the same sign. This

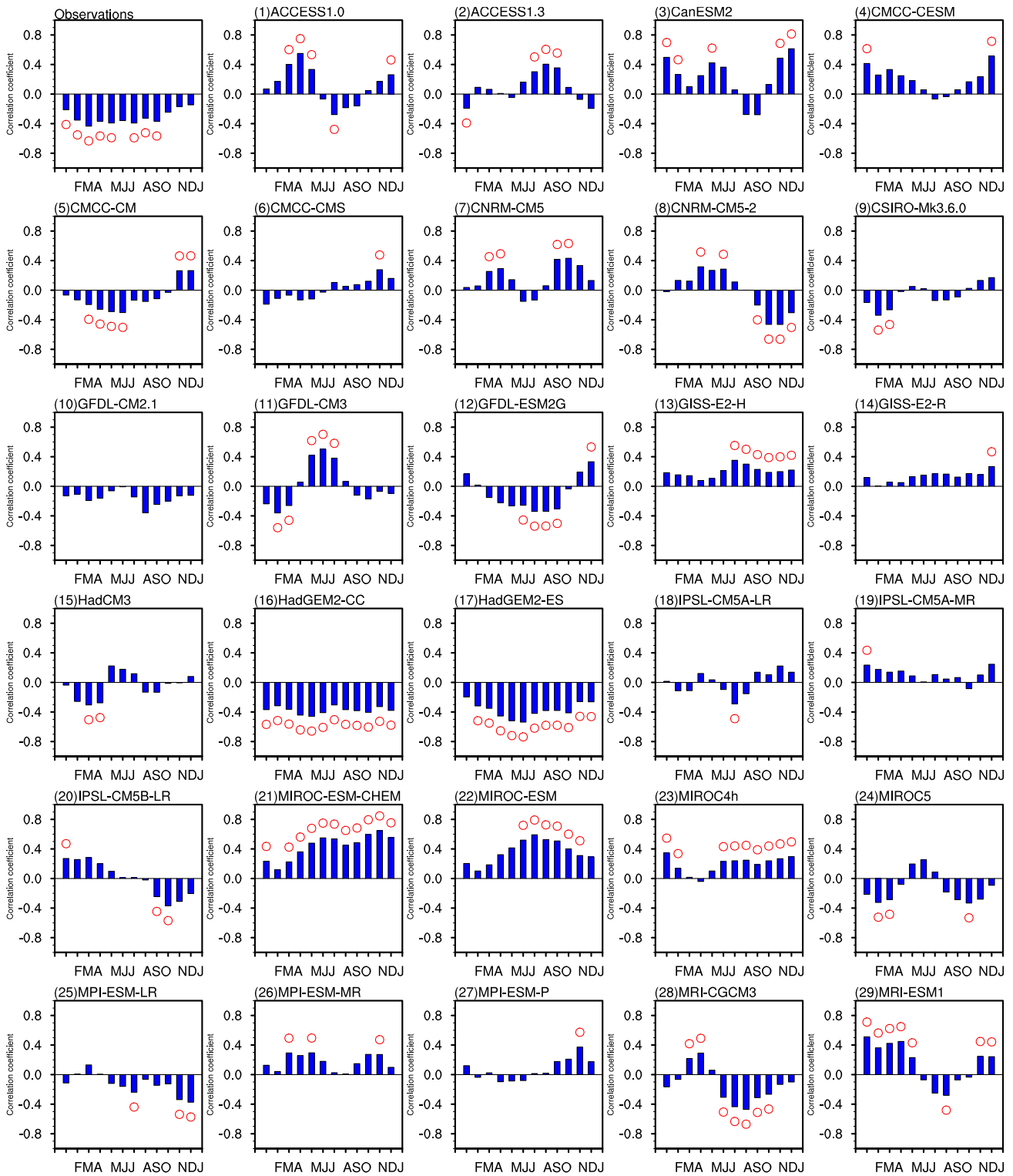
rules out models with the opposite sensible heat flux trends to the reanalysis product in most parts of the plateau, such as the MIROC-ESM and MPI-ESM-LR models. The sensible heat flux trend in the HadGEM2-CC and HadGEM2-ES models is highly and positively correlated with the trend in the reanalysis product at all altitudes. The correlation coefficients from low to high elevation almost all exceed the 99% confidence level. Therefore, the HadGEM2-CC and HadGEM2-ES models are consistently the best simulations of the sensible heat flux trend over the Tibetan Plateau at all altitudes.

Figure 7 shows the topography of the Tibetan Plateau in the reanalysis product and the 29 CMIP5 climate models and Figure 8 shows the Taylor diagrams for the elevation over the Tibetan Plateau in 1000 m wide altitudinal bands between the CMIP5 models and the reanalysis product. The HadGEM2-CC and HadGEM2-ES have a good skill for showing the terrain over the Tibetan Plateau at all altitudes (Figure 7). The spatial correlation coefficients for altitude between the reanalysis product and each of the two models exceed 0.9 in every 1,000 m wide altitudinal band (Figure 8). Because these two models have better simulation skills for both the sensible heat flux trend and altitude, the coherence of the elevation-dependent variation in the sensible heat flux trend between the observations and these two models (Figures 3 and 4) is not fortuitous. The ACCESS1.0 and ACCESS1.3 models, which had a poor performance in simulating the decreasing sensible heat flux trend, showed good skills in depicting the altitude over the Tibetan Plateau. They may indicate that an accurate analogue for topographic altitude is a major requisite for models simulating the sensible heat flux trend over the Tibetan Plateau, but it may not be sufficient.

## 4.2 | Reasons for the good performance of the HadGEM2-CC and HadGEM2-ES models

We investigated why the HadGEM2-CC and HadGEM2-ES models have better skills in simulating the elevation-dependence of the sensible heat flux trend than the other models in CMIP5. The topography, which exerts a primary control on the total precipitation in mountain regions (e.g., Daly *et al.*, 1994; Frei and Schär, 1998; Wastl and Zängl, 2008), is an important, but not the major, factor influencing the biases and skills of models in simulating the sensible heat flux trend. Finding and quantifying the dominant factor influencing the dependence of the sensible heat flux trend on elevation in data is affected by the uncertainties in the parameterization scheme for sensible heat, which is intricate and





**FIGURE 4** Correlation coefficients between the sensible heat flux trend and elevation for the observations and the 29 climate models in CMIP5 over the Tibetan Plateau during the time period 1980–2005. The red open circles represent values exceeding the 90% significance level

may vary between the different models in CMIP5. Based on the previous studies, the sensible heat flux is sensitive to the variables of land surface processes, such as the surface wind speed, the difference in temperature between

the ground and the air (e.g., Yeh and Gao, 1979; Chen *et al.*, 1985; Li *et al.*, 2001; Duan and Wu, 2008; Duan *et al.*, 2011, 2013; Cui *et al.*, 2015; Zhu *et al.*, 2017; Zhu *et al.*, 2019), snow cover (e.g., Vernekar *et al.*, 1995;

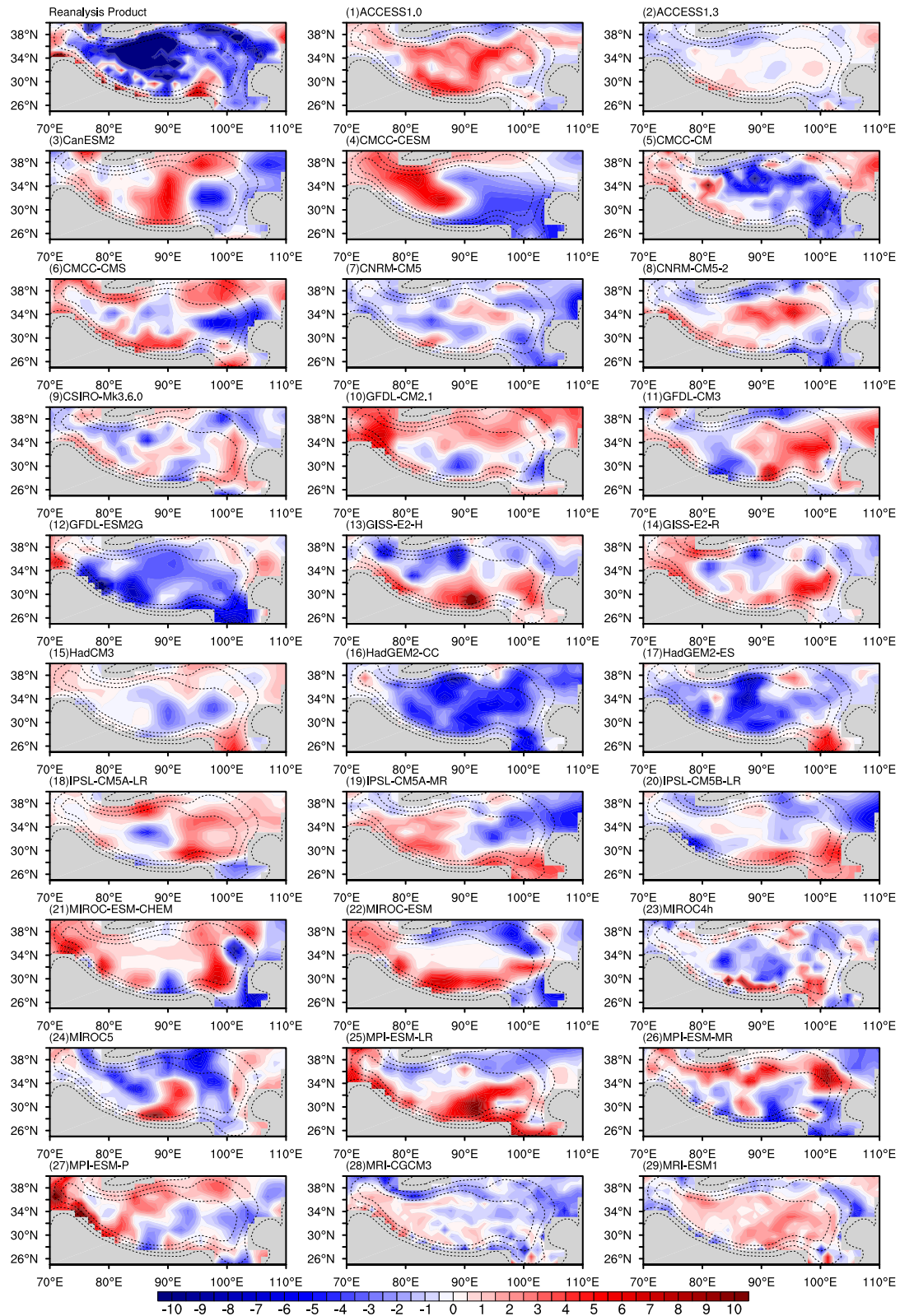


**FIGURE 5** Linear variation of the sensible heat in the reanalysis product and 29 climate models of CMIP5 over the Tibetan Plateau above 1,000 m in spring during the time period 1980–2005. Units:  $\text{W m}^{-2} (10 \text{ yr})^{-1}$ . The black dashed lines indicate the elevation levels of 1,000, 2,000, 3,000, and 4,000 m, respectively

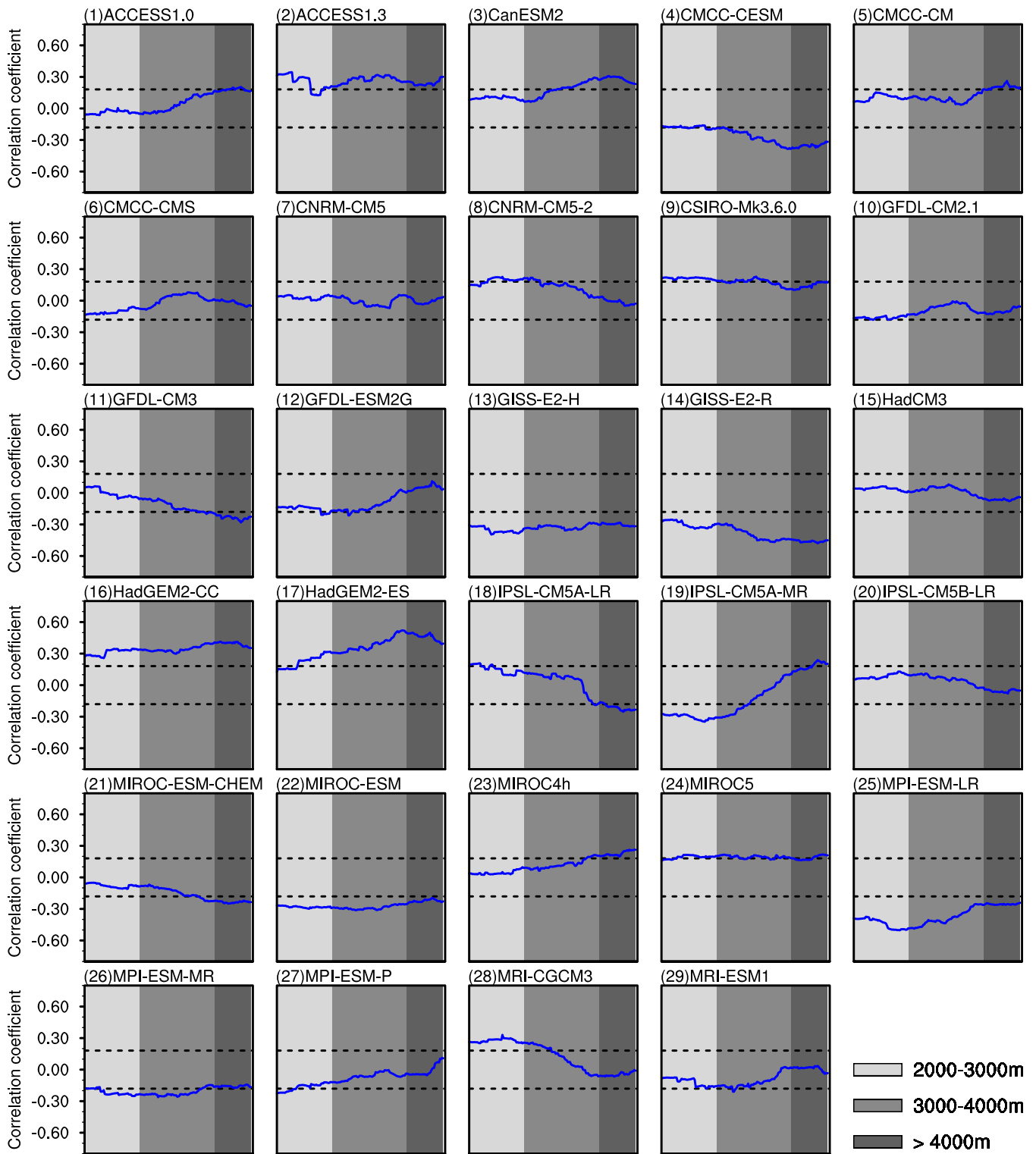


**FIGURE 6** The blue lines show the correlation coefficients for the sensible heat flux trends between the reanalysis product and the 29 models in CMIP5. The correlation coefficients were calculated, based on every successive 201 samples ordered from low to high elevation. The correlation coefficients were multiplied by either 1 or  $-1$  depending on whether the average sensible heat flux trend over the Tibetan Plateau in spring in the reanalysis product and models had the same or different signs. The range of average altitude for each sample group ( $n = 201$ ) is expressed in grey. The black dashed line indicates the 99% significance level

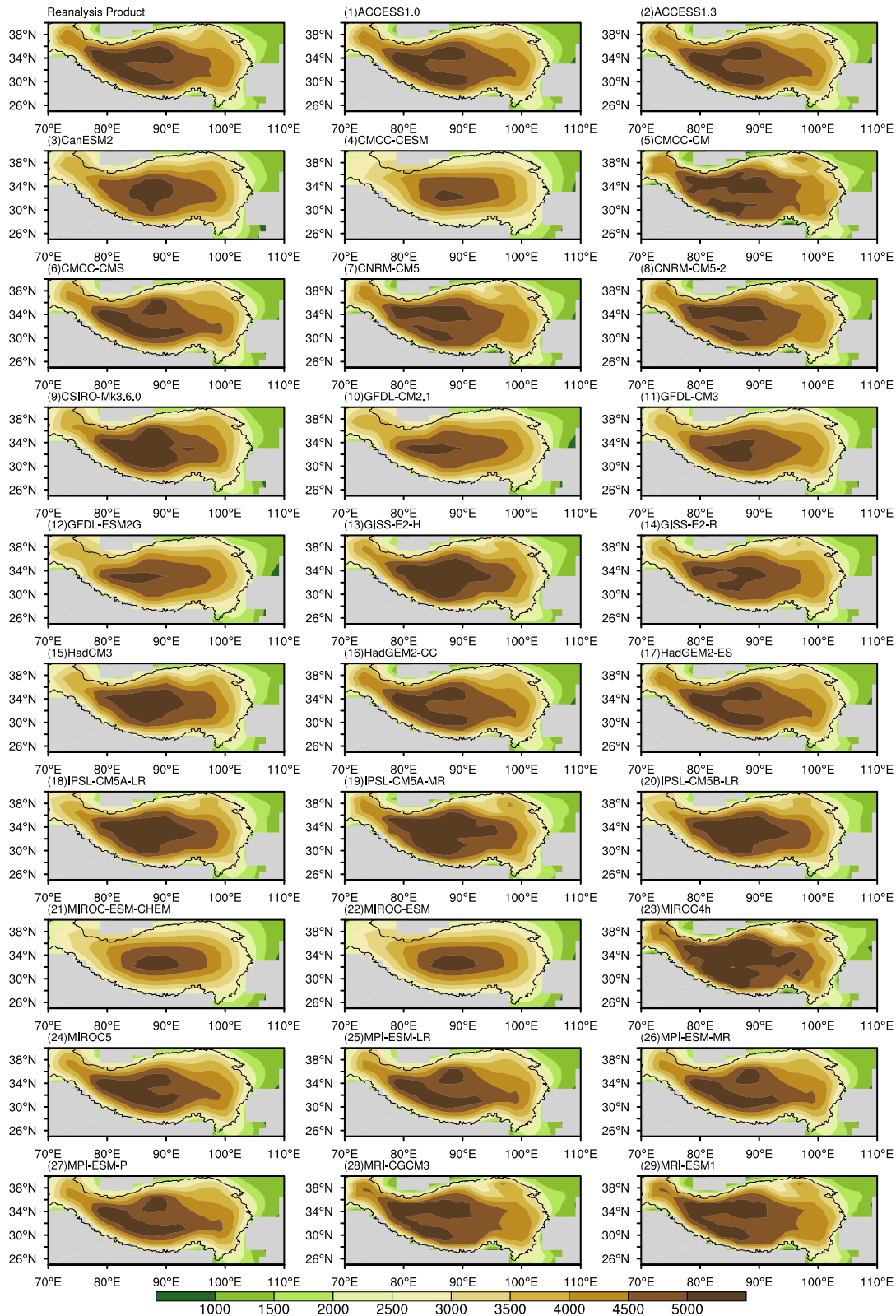


**FIGURE 7** Topographic altitude of the reanalysis product and 29 climate models in CMIP5 over the Tibetan Plateau above 1,000 m. Units: m

Zhang and Tao, 2001; Wang *et al.*, 2018) and the leaf area index (LAI; Mamkin *et al.*, 2016; Safa *et al.*, 2018). Correlation and regression analysis are usually used to find

possible linear relationships between two variables. To capture the key factor affecting the simulation result for sensible heat in models with good performance, the

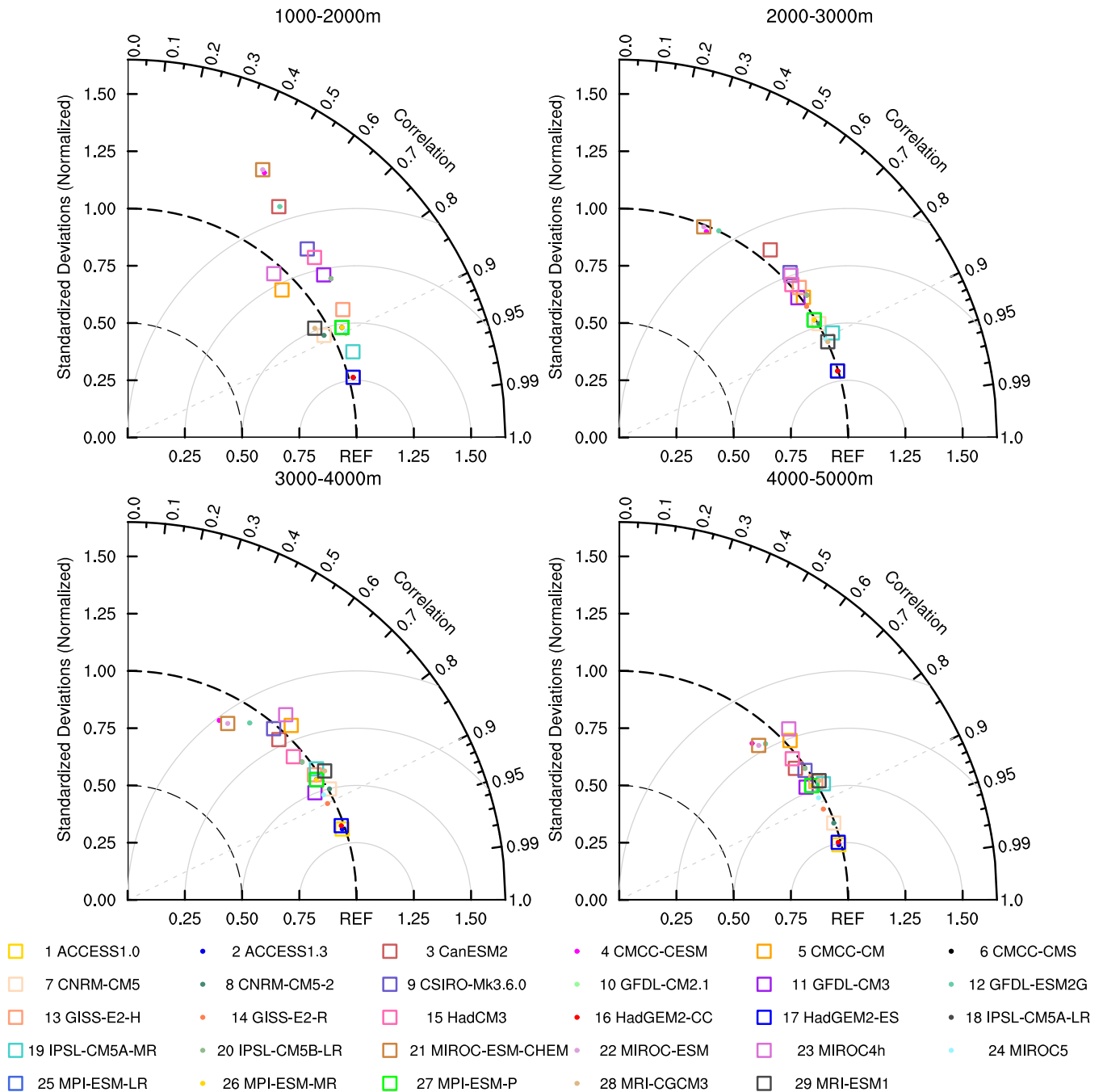


**FIGURE 8** Taylor diagrams for elevation over the Tibetan Plateau in 1,000 m wide altitudinal bands between the CMIP5 models and the reanalysis product

responses of the sensible heat flux to the surface wind speed, the difference in temperature between the surface and the air, the LAI and the surface snow amount (SNW) have been determined via regression analysis.

We analysed the effect of the difference in surface air temperature and surface wind speed on the dependence of the sensible heat flux trend on elevation in the 29 CMIP5 models. The comparison of the linear variation rates for the surface wind speed and the difference in temperature between the ground and the air derived

from JRA25 reanalysis dataset and simulation in the 29 CMIP5 models are shown in Figures 9 and 10, respectively. Prior to that, we evaluate the representation of surface wind and temperature in the reanalysis against observations. The correlation coefficients between the domain-averaged surface 2 m air temperature, soil temperature and surface 10 m wind speed over the eastern Tibetan Plateau (25°–40°N, 90°–110°E) above 1,000 m from the JRA25 reanalysis dataset and the 124-station-averaged corresponding variables of the eastern Tibetan

Plateau from the observations during spring are 0.98, 0.53, and 0.61, respectively, which are all significant at the 90% confidence level.

In addition, the product of the wind speed at 10 m ( $V_0$ ) and the difference in temperature between the ground and the air ( $T_s - T_a$ ) is described by  $H_{VT}$ :

$$H_{VT} = V_0 (T_s - T_a) \quad (2)$$

The pattern of the sensible heat regressed on  $H_{VT}$  at the corresponding point in each model is shown in Figure 11. The regression coefficients were multiplied by either 1 or  $-1$  depending on the trend in  $H_{VT}$  was positive or negative. As a result of the absence of the surface wind speed in the model output of GFDL-CM2.1, there is a blank space in Figure 9 (10) and Figure 11 (10), which is retained for the convenience of comparison.

Almost all models in CMIP5 are unable to simulate the linear trend in the difference of temperature between the ground surface and the air and the surface wind speed, characterized by a weaker or even opposite trend in part of, or the whole, plateau compared with the reanalysis product. The results presented in Figure 11 show that the two variables of surface wind speed and the difference in temperature between the ground and the air are the dominant factors in the evolution of the sensible heat flux in most models. In these models, the regression field of the sensible heat against  $H_{VT}$  approximates the variation in the sensible heat flux in Figure 5 and the pattern correlation coefficients between the regression field and the distribution of the sensible heat flux trend in the corresponding model in Figure 5 mostly exceed 0.5 or even 0.8 (at the 99% confidence level). This indicates that the sensible heat flux in these models is sensitive to the variations in the surface wind speed and the difference of temperature between the ground and the air, in addition to their biases deviating from the reanalysis product. More significantly, in the HadGEM2-CC and HadGEM2-ES models, which possess good skills in depicting the elevation-dependent sensible heat flux trend, the fraction of the variation in the sensible heat flux influenced by the surface wind speed and the difference in temperature between the ground and the air is not the most important factor. These models avoid the biases in the sensible heat flux trend arising from the imprecise simulation of the difference in temperature between the ground and the air and surface wind speed.

We therefore tried to determine the factor with the predominant role in the variation of the sensible heat flux trend with elevation in the HadGEM2-CC and HadGEM2-ES models. The LAI and SNW influence the albedo of the Earth's surface and thereby the net

radiation flux available to drive the latent and sensible heat. In addition, the LAI and SNW influence the partitioning of the net radiation flux between the latent and sensible heat (e.g., Verstraete and Dickinson 1986; Wang et al. 2018). Hence, the responses of the sensible heat flux to the LAI and SNW in the HadGEM2-CC and HadGEM2-ES models have been demonstrated in Figure 12. In the HadGEM2-CC and HadGEM2-ES models, the regression patterns of the sensible heat flux against the LAI at corresponding points (Figure 12) are very similar to the distribution of the sensible heat flux trend of the relevant model in Figure 5, and the pattern correlation coefficients between the regression field and the linear variation rate of the sensible heat flux in the relevant model in Figure 5 both exceed 0.8 (at the 99% confidence level). In contrast, the response fields of the sensible heat against SNW in the HadGEM2-CC and HadGEM2-ES models appear inconsistent variation with the sensible heat flux trend in Figure 5, with the pattern correlation coefficients below 0.36. This indicates that the sensible heat flux in these two models is sensitive to the variations in leaf area index. Maybe the parameterization scheme of vegetation plays a role for these two models in simulating the elevation-dependent sensible heat flux trend. Unlike previous Hadley Centre coupled climate-carbon cycle simulations (e.g., Cox *et al.*, 2000; Freidlingstein *et al.*, 2006) that used a static agricultural mask, the Top-down Representation of Interactive Foliage and Flora Including Dynamics (TRIFFID) dynamic global vegetation scheme has now been updated to allow time-varying land-use distributions in the CMIP5 simulations (Cox, 2001; Collins *et al.*, 2011; Jones *et al.*, 2011). The result above shows that the LAI is the predominant factor affecting the variation of the sensible heat flux trend with elevation in the HadGEM2-CC and HadGEM2-ES models in CMIP5, which include the implementation of a dynamic vegetation model.

## 5 | SUMMARY AND DISCUSSION

The dependence of the sensible heat flux trend on elevation has been poorly investigated in previous studies. The analysis should be conducted using multiple datasets (e.g., observations, atmospheric reanalysis dataset and models) to confirm the conclusions drawn from the observations, to evaluate the simulation performance of the models and to further overcome the limitations resulting from the sparseness of in situ stations in data-poor high-altitude regions. The analyses in this study reveal a consistent variation of the sensible heat flux trend with elevation over the Tibetan Plateau in both the observational and reanalysis datasets. We also evaluated

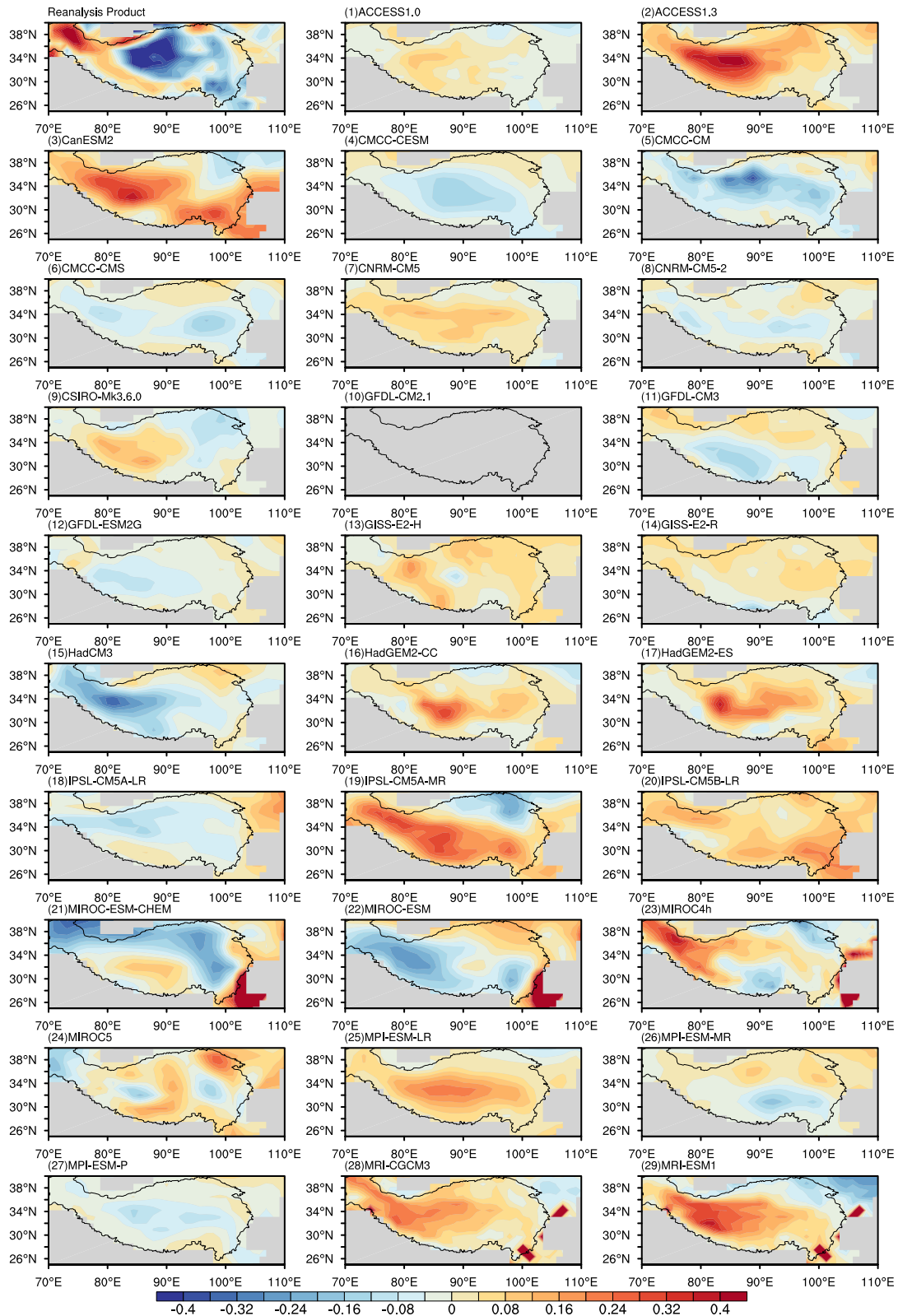


**FIGURE 9** Linear variation rate for the surface wind speed in the reanalysis product and the 29 CMIP5 climate models over the Tibetan Plateau above 1,000 m in spring during the time period 1980–2005. The surface wind speed is absent from the model output in GFDL-CM2.1. Units:  $\text{m s}^{-1} (10 \text{ yr})^{-1}$

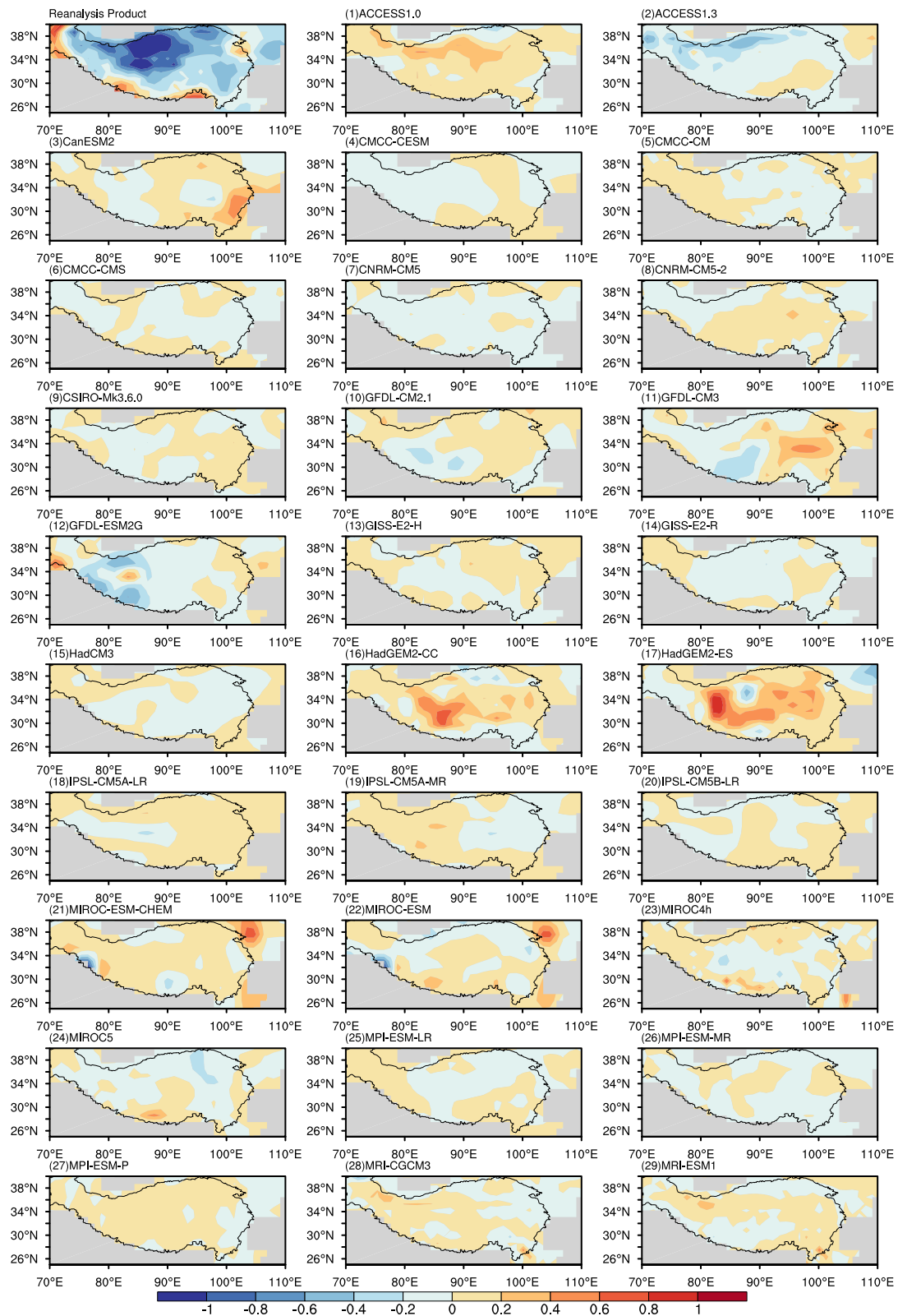


**FIGURE 10** Linear variation rate for the difference in temperature between the ground and the air for the reanalysis product and the 29 CMIP5 climate models over the Tibetan Plateau above 1,000 m in spring during the time period 1980–2005. Units:  $^{\circ}\text{C} (10 \text{ yr})^{-1}$



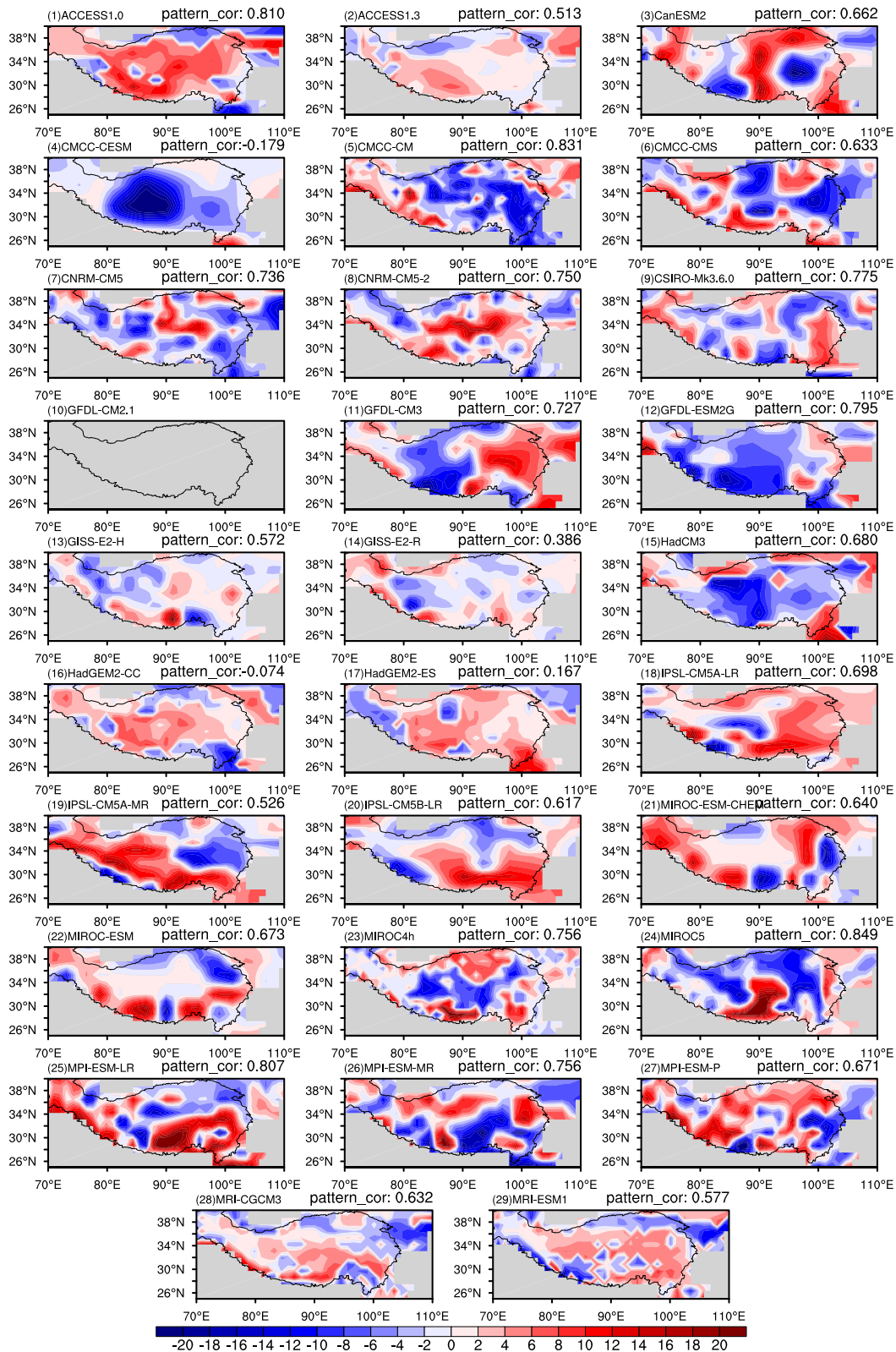


**FIGURE 11** Regression field of sensible heat against  $H_{VT}$  at the corresponding point over the Tibetan Plateau above 1,000 m in the 29 CMIP5 climate models in spring during the time period 1980–2005. The surface wind speed is absent from the model output in GFDL-CM2.1. The values have been multiplied by either 1 or  $-1$  depending on the positive or negative trends in  $H_{VT}$ . The pattern correlation coefficient between the regression field and distribution of the sensible heat flux trend in the corresponding model in Figure 5 is given in the upper right-hand corner of each graph. Units:  $W m^{-2}$

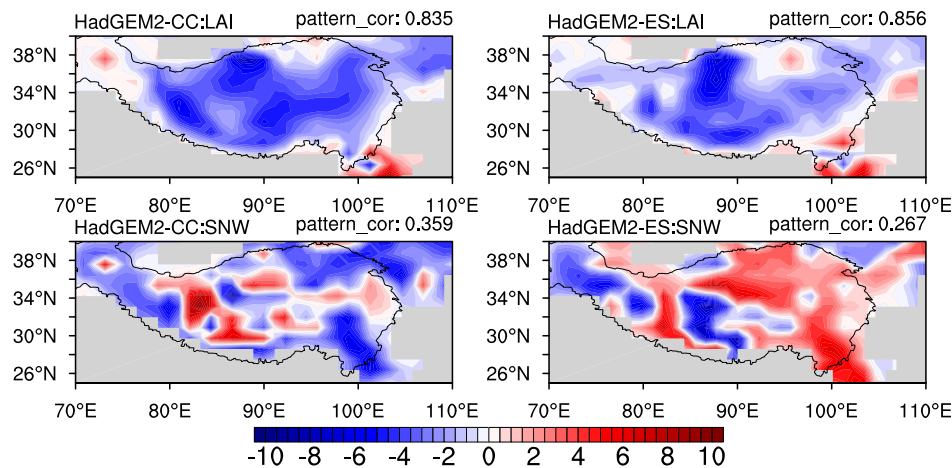


**FIGURE 12** Regression field of the sensible heat against the LAI and SNW at corresponding point over the Tibetan Plateau above 1,000 m in the HadGEM2-CC and HadGEM2-ES models of CMIP5 in spring during the time period 1980–2005. The values have been multiplied by either 1 or  $-1$  depending on the positive or negative trends in LAI or SNW. The pattern correlation coefficient between the regression field and the distribution of the sensible heat flux trend of the corresponding model in Figure 5 is given in the upper right-hand corner of each graph. Units:  $\text{W m}^{-2}$

the performance of the climate models in CMIP5 in simulating the elevation-dependent sensible heat flux trend by comparing their outputs with ground observations. We considered the main factors influencing the analogue capability. Several of our findings will benefit future studies in mountainous regions.

The sensible heat flux trend over the Tibetan Plateau shows a dependence on elevation in both the observational and reanalysis datasets. This dependency is characterized by a larger negative trend at higher altitudes and confirms the conclusions of Zhu *et al.* (2019). Most of the models in CMIP5 are unable to capture the weakening sensible heat flux trends in high-altitude regions and the dependence on elevation. Fortunately, two of the 29 CMIP5 models showed an excellent performance in simulating the decreasing trend in sensible heat flux over the Tibetan Plateau over the most prominent elevation ranges and seasons. In these two models, the sensible heat flux trend was significantly negatively correlated with the elevation in most seasons. The models with good skills were also consistently excellent simulators of the sensible heat flux trend in both low or high elevation regions of the Tibetan Plateau. The models that reproduce the dependence on elevation in the sensible heat flux trend also perform well in depicting the terrain over the Tibetan Plateau at all altitudes. Whereas other climate models such as ACCESS1.0 and ACCESS1.3 show a realistic topography but still perform poorly in reproducing the observed sensible heat flux trend over the Tibetan Plateau. This suggests that a realistic topography might be a necessary, but not sufficient, condition for simulating the dependence of the sensible heat flux trend on elevation.

In most models, the difference in temperature between the ground and the air and the surface wind speed are the key factors affecting the evolution of the sensible heat flux, although these two factors present large biases deviating from the reanalysis product in almost all the models in this study. We found that the LAI, rather than the difference in temperature between the ground and the air, the surface wind speed and the surface snow amount, plays the predominant role in affecting the dependence of the sensible heat flux trend on elevation in the models with a good simulation performance, primarily the HadGEM2-CC and HadGEM2-ES models. This may be related to the dynamic vegetation scheme in these two models. It requires further investigation.

In addition, some models analysed in this study do not define surface temperatures in soil, but as skin temperatures for the relative areas of different surface types, such as soil, inland water, snow or canopy of a thin layer close to the surface. The complexity in modelling physical processes at the land surface boundary exerts influence on the CMIP5 model evaluation of the ground-air temperature differences (Garcia-Garcia *et al.*, 2019).

The terrain of the Tibetan Plateau is extremely complex. Special efforts should be made to decrease uncertainties in mountain areas—for instance, expanding the surface climate observational network to cover higher altitude regions ( $>4,000$  m), extending the duration of data collection and improving the spatial resolution in models. Limitations in the available data make it extremely difficult to determine the dependency of climate variables on elevation in high-altitude regions (Rangwala and Miller, 2012; Pepin *et al.*, 2015).

Understanding how future variations in climate may affect the redistribution of energy, the hydrological cycle, and the zonation of ecosystems in high-mountain regions provide a compelling argument for studying this difficult issue further.

## ACKNOWLEDGEMENTS

The authors thank the China Meteorological Administration for kindly providing the observational data and thank Dr Yongjie Huang (Institute of Atmospheric Physics/Chinese Academy of Sciences) for providing the map database. The authors also thank the anonymous reviewers and editor for their useful comments. This work was supported by Sichuan Science and Technology Program (2019YJ0359, 2019YJ0362), Foundation for Innovative Research Groups of the National Natural Science Foundation of China, Innovative Research Group Project of the National Natural Science Foundation of China (41831175, 42075019, 91937302, 41721004, 41975130), the Heavy Rain and Drought-Flood Disasters in Plateau and Basin Key Laboratory of Sichuan Province (SZKT201906), the Sichuan Provincial Department of Education Project of China (15ZB0170) and the Strategic Priority Research Program of the Chinese Academy of Sciences (XDA20060501).

## ORCID

Gang Huang  <https://orcid.org/0000-0002-8692-7856>

## REFERENCES

- Boos, W.R. and Kuang, Z. (2010) Dominant control of the South Asian monsoon by orographic insulation versus plateau heating. *Nature*, 463, 218–222.
- Chakraborty, A., Nanjundiah, R.S. and Srinivasan, J. (2002) Role of Asian and African orography in Indian summer monsoon. *Geophysical Research Letters*, 29(20), 1989–50-4. <https://doi.org/10.1029/2002GL015522>.
- Chakraborty, A., Nanjundiah, R.S. and Srinivasan, J. (2006) Theoretical aspects of the onset of Indian summer monsoon from perturbed orography simulations in a GCM. *Annales de Geophysique*, 24, 2075–2089.
- Chen, L.X., Reiter, E.R. and Feng, Z.Q. (1985) The atmospheric heat source over the Tibetan Plateau: May–August 1979. *Monthly Weather Review*, 113, 1771–1790. [https://doi.org/10.1175/1520-0493\(1985\)113<1771:TAHSOT>2.0.CO;2](https://doi.org/10.1175/1520-0493(1985)113<1771:TAHSOT>2.0.CO;2).
- Collins, W.J., Bellouin, N., Doutriaux-Boucher, M., Gedney, N., Halloran, P., Hinton, T., Hughes, J., Jones, C.D., Joshi, M., Liddicoat, S., Martin, G., O'Connor, F., Rae, J., Senior, C., Sitch, S., Totterdell, I., Wiltshire, A. and Woodward, S. (2011) Development and evaluation of an EarthSystem model—HadGEM2. *Geoscientific Model Development*, 4(4), 1051–1075. <https://doi.org/10.5194/gmd-4-1051-2011>.
- Cox, P., Betts, R., Jones, C., Spall, S. and Totterdell, I. (2000) Acceleration of global warming due to carbon-cycle feedbacks in a coupled climate model. *Nature*, 408, 184–187.
- Cox P. 2001 Description of the TRIFFID dynamic global vegetation model. Hadley Centre Technical Note 24, Met Office, UK.
- Cui, Y.F., Duan, A.M., Liu, Y.M. and Wu, G.X. (2015) Interannual variability of the spring atmospheric heat source over the Tibetan Plateau forced by the North Atlantic SSTA. *Climate Dynamics*, 45, 1617–1634. <https://doi.org/10.1007/s00382-014-2417-9>.
- Daly, C., Neilson, R.P. and Phillips, D.L. (1994) A statistical-topographic model for mapping climatological precipitation over mountainous terrain. *Journal of Applied Meteorology*, 33, 140–158.
- Dee, D.P., Uppala, S.M., Simmons, A.J., Berrisford, P., Poli, P., Kobayashi, S., Andrae, U., Balmaseda, M.A., Balsamo, G., Bauer, P., Bechtold, P., ACM, B., Van De Berg, L., Bidlot, J., Bormann, N., Delsol, C., Dragani, R., Fuentes, M., Geer, A.J., Haimberger, L., Healy, S.B., Hersbach, H., Hólm, E.V., Isaksen, I., Kållberg, P., Köhler, M., Matricardi, M., AP, M.N., Monge-Sanz, B.M., Morcrette, J.J., Park, B.K., Peubey, C., De Rosnay, P., Tavolato, C., Thépaut, J.-N. and Vitart, F. (2011) The ERA-Interim reanalysis: configuration and performance of the data assimilation system. *Quarterly Journal of the Royal Meteorological Society*, 137, 553–597. <https://doi.org/10.1002/qj.828>.
- Duan, A.M. and Wu, G.X. (2005) Role of the Tibetan Plateau thermal forcing in the summer climate patterns over subtropical Asia. *Climate Dynamics*, 24, 793–807. <https://doi.org/10.1007/s00382-004-0488-8>.
- Duan, A.M. and Wu, G.X. (2008) Weakening trend in the atmospheric heat source over the Tibetan Plateau during recent decades. Part I: observations. *Journal of Climate*, 21, 3149–3164. <https://doi.org/10.1175/2007JCLI1912.1>.
- Duan, A.M., Li, F., Wang, M.R. and Wu, G.X. (2011) Persistent weakening trend in the spring sensible heat source over the Tibetan Plateau and its impact on the Asian summer monsoon. *Journal of Climate*, 24, 5671–5682. <https://doi.org/10.1175/JCLI-D-11-00052.1>.
- Duan, A.M., Wu, G.X., Liu, Y.M., Ma, Y.M. and Zhao, P. (2012) Weather and climate effects of the Tibetan Plateau. *Advances in Atmospheric Sciences*, 29, 978–992. <https://doi.org/10.1007/s00376-012-1220-y>.
- Duan, A.M., Wang, M.R., Lei, Y.H. and Cui, Y.F. (2013) Trends in summer rainfall over China associated with the Tibetan Plateau sensible heat source during 1980–2008. *Journal of Climate*, 26, 261–275. <https://doi.org/10.1175/JCLI-D-11-00669.1>.
- Flohn, H. (1957) Large-scale aspects of the summer monsoon in South and East Asia. *Journal of the Meteorological Society of Japan*, 35, 180–186.
- Flohn, H. 1960. Recent investigations on the mechanism of the ‘Summer Monsoon’ of Southern and Eastern Asia. In *Proceedings of Symposium on Monsoons of the World*
- Frei, C. and Schär, C. (1998) A precipitation climatology of the Alps from high-resolution rain-gauge observations. *International Journal of Climatology*, 18, 873–900.
- Friedlingstein, P., Cox, P., Betts, R., Bopp, L., von Bloh, W., Brovkin, V., Cadule, P., Doney, S., Eby, M., Fung, I., Bala, G., John, J., Jones, C., Joos, F., Kato, T., Kawamiya, M., Knorr, W., Lindsay, K., Matthews, H.D., Raddatz, T., Rayner, R., Reick, C., Roeckner, E., Schnitzler, K.G., Schnur, R., Strassmann, K., Weaver, A.J., Yoshikawa, C. and Zeng, N. (2006) Climate-carbon cycle feedback analysis: results from the C<sup>4</sup>MIP model

- intercomparison. *Journal of Climate*, 19(14), 3337–3353. <https://doi.org/10.1175/JCLI3800.1>.
- García-García, A., Cuesta-Valero, F.J., Beltrami, H. and Smerdon, J. E. (2019) Characterization of air and ground temperature relationships within the CMIP5 historical and future climate simulations. *Journal of Geophysical Research: Atmospheres*, 124, 3903–3929. <https://doi.org/10.1029/2018JD030117>.
- Hu, S. and Boos, W.R. (2017a) The physics of orographic elevated heating in radiative-convective equilibrium. *Journal of the Atmospheric Sciences*, 74(9), 2949–2965. <https://doi.org/10.1175/JAS-D-16-0312.1>.
- Hu, S. and Boos, W.R. (2017b) Competing effects of surface albedo and orographic elevated heating on regional climate. *Geophysical Research Letters*, 44(13), 6966–6973. <https://doi.org/10.1002/2016GL072441>.
- Immerzeel, W.W., Van Beek, L.P.H. and Bierkens, M.F.P. (2010) Climate change will affect the Asian water towers. *Science*, 328(5984), 1382–1385. <https://doi.org/10.1126/science.1183188>.
- Jones, C.D., Hughes, J.K., Bellouin, N., Hardiman, S.C., Jones, G.S., Knight, J., Liddicoat, S., O'Connor, F.M., Andres, R.J., Bell, C., Boo, K.O., Bozzo, A., Butchart, N., Cadule, P., Corbin, K.D., Doutriaux-Boucher, M., Friedlingstein, P., Gornall, J., Gray, L., Halloran, P.R., Hurtt, G., Ingram, W.J., Lamarque, J.F., Law, R. M., Meinshausen, M., Osprey, S., Palin, E.J., Parsons Chini, L., Raddatz, T., Sanderson, M.G., Sellar, A.A., Schurer, A., Valdes, P., Wood, N., Woodward, S., Yoshioka, M. and Zerroukat, M. (2011) The HadGEM2-ES implementation of CMIP5 centennial simulations. *Geoscientific Model Development*, 4(3), 543–570. <https://doi.org/10.5194/gmd-4-543-2011>.
- Kalnay, E., Kanamitsu, M., Kistler, R., Collins, W., Deaven, D., Gandin, L., Iredell, M., Saha, S., White, G., Woollen, J., Zhu, Y., Chelliah, M., Ebisuzaki, W., Higgins, W., Janowiak, J., Mo, K.C., Ropelewski, C., Wang, J., Leetmaa, A., Reynolds, R., Jenne, R. and Joseph, D. (1996) The NCEP/NCAR 40-year reanalysis project. *Bulletin of the American Meteorological Society*, 77, 437–470.
- Kanamitsu, M., Ebisuzaki, W., Woollen, J., Yang, S.K., Hnilo, J.J., Fiorino, M. and Potter, G.L. (2002) NCEP-DOE AMIP-II Reanalysis (R-2). *Bulletin of the American Meteorological Society*, 83, 1631–1643.
- Li, C.F. and Yanai, M. (1996) The onset and interannual variability of the Asian summer monsoon in relation to land-sea thermal contrast. *Journal of Climate*, 9, 358–375.
- Li, W.P., Wu, G.X., Liu, Y.M. and Liu, X. (2001) How the surface processes over the Tibetan Plateau affect the summertime Tibetan Anticyclone-numerical experiments. *Chinese Journal of Atmospheric Sciences*, 25(6), 809–816. <https://doi.org/10.3878/j.issn.1006-9895.2001.06.08> (in Chinese with English abstract).
- Liu, Y.M., Wu, G.X., Hong, J.L., Dong, B., Duan, A.M., Bao, Q. and Zhou, L.J. (2012) Revisiting Asian monsoon formation and change associated with Tibetan Plateau forcing: II. Change. *Climate Dynamics*, 39, 1183–1195. <https://doi.org/10.1007/s00382-012-1335-y>.
- Liu, B.Q., Wu, G.X., Mao, J.Y. and He, J.H. (2013) Genesis of the South Asian high and its impact on the Asian summer monsoon onset. *Journal of Climate*, 26, 2976–2991. <https://doi.org/10.1175/JCLI-D-12-00286.1>.
- Mamkin, V., Kurbatova, J., Avilov, V., Mukhartova, Y., Krupenko, A., Ivanov, D., Levashova, N. and Olchev, A. (2016) Changes in net ecosystem exchange of CO<sub>2</sub>, latent and sensible heat fluxes in a recently clear-cut spruce forest in western Russia: results from an experimental and modeling analysis. *Environmental Research Letters*, 11(12), 125012. <https://doi.org/10.1088/1748-9326/aa5189>.
- Molnar, P. and Emanuel, K.A. (1999) Temperature profiles in radiative-convective equilibrium above surfaces at different heights. *Journal of Geophysical Research-Atmospheres*, 104 (D20), 24265–24271. <https://doi.org/10.1029/1999JD900485>.
- Onogi, K., Tsutsui, J., Koide, H., Sakamoto, M., Kobayashi, S., Hatsushika, H., Matsumoto, T., Yamazaki, N., Kamahori, H., Takahashi, K., Kadokura, S., Wada, K., Kato, K., Oyama, R., Ose, T., Mannoji, N. and Taira, R. (2007) The JRA-25 Reanalysis. *Journal of the Meteorological Society of Japan*, 85(3), 369–432.
- Pepin, N., Bradley, R.S., Diaz, H.F., Baraer, M., Caceres, E.B., Forsythe, N., Fowler, H., Greenwood, G., Hashmi, M.Z., Liu, X. D., Miller, J.R., Ning, L., Ohmura, A., Palazzi, E., Rangwala, I., Schöner, W., Severskiy, I., Shahgedanova, M., Wang, M.B., Williamson, S.N. and Yang, D.Q. (2015) Elevation-dependent warming in mountain regions of the world. *Nature Climate Change*, 5, 424–430. <https://doi.org/10.1038/NCLIMATE2563>.
- Rangwala, I. and Miller, J.R. (2012) Climate change in mountains: a review of elevation-dependent warming and its possible causes. *Climatic Change*, 114, 527–547. <https://doi.org/10.1007/s10584-012-0419-3>.
- Safa, B., Arkebauer, T.J., Zhu, Q., Suyker, A. and Irmak, S. (2018) Latent heat and sensible heat flux simulation in maize using artificial neural networks. *Computers and Electronics in Agriculture*, 154, 155–164. <https://doi.org/10.1016/j.compag.08.038>.
- Verstraete, M. and Dickinson, R. (1986) Modeling surface processes in atmospheric general circulation models. *Annales de Geophysique*, 4(4), 357–364.
- Vernekar, A.D., Zhou, J. and Shukla, J. (1995) The effect of Eurasian snow cover on the Indian monsoon. *Journal of Climate*, 8(2), 248–266. [https://doi.org/10.1175/1520-0442\(1995\)008<0248:TEOESC>2.0.CO;2](https://doi.org/10.1175/1520-0442(1995)008<0248:TEOESC>2.0.CO;2).
- Viviroli, D., Dürr, H.H., Messerli, B., Meybeck, M. and Weingartner, R. (2007) Mountains of the world, water towers for humanity: typology, mapping, and global significance. *Water Resources Research*, 43(7), 1–13.
- Wan, R.J. and Wu, G.X. (2007) Mechanism of the spring persistent rains over southeastern China. *Science in China Series D: Earth Sciences*, 50, 130–144. <https://doi.org/10.1007/s11430-007-2069-2>.
- Wan, R.J., Zhao, B.K. and Wu, G.X. (2009) New evidences on the climatic causes of the formation of the spring persistent rains over southeastern China. *Advances in Atmospheric Sciences*, 26, 1081–1087. <https://doi.org/10.1007/s00376-009-7202-z>.
- Wang, Z.Q., Duan, A.M. and Wu, G.X. (2014) Time-lagged impact of spring sensible heat over the Tibetan Plateau on the summer rainfall anomaly in East China: case studies using the WRF model. *Climate Dynamics*, 42, 2885–2898. <https://doi.org/10.1007/s00382-013-1800-2>.
- Wang, Z.B., Wu, R.G., Chen, S.F., Huang, G., Liu, G. and Zhu, L.H. (2018) Influence of western Tibetan Plateau summer snow cover on East Asian summer rainfall. *Journal of Geophysical Research-Atmospheres*, 123(5), 2371–2386. <https://doi.org/10.1002/2017JD028016>.

- Wastl, C. and Zängl, G. (2008) Analysis of mountain-valley precipitation differences in the Alps. *Meteorologische Zeitschrift*, 17(3), 311–321.
- Wu, G.X., Li, W.P. and Guo, H. (1997) Sensible heat driven air-pump over the Tibetan-Plateau and its impacts on the Asian Summer Monsoon. In: Ye, D.Z. (Ed.) *Collections on the Memory of Zhao Jiuzhang*. Beijing: Science Press, pp. 116–126 (in Chinese).
- Wu, G.X., Liu, Y.M., Wang, T.M., Wan, R.J., Liu, X., Li, W.P., Wang, Z.Z., Zhang, Q., Duan, A.M. and Liang, X.Y. (2007) The influence of mechanical and thermal forcing by the Tibetan Plateau on Asian climate. *Journal of Hydrometeorology*, 8, 770–789. <https://doi.org/10.1175/JHM609.1>.
- Wu, G.X., Liu, Y.M., He, B., Bao, Q., Duan, A.M. and Jin, F.F. (2012a) Thermal controls on the Asian summer monsoon. *Scientific Reports*, 2, 404. <https://doi.org/10.1038/srep00404>.
- Wu, G.X., Liu, Y.M., Dong, B.W., Liang, X.Y., Duan, A.M., Bao, Q. and Yu, J.J. (2012b) Revisiting Asian monsoon formation and change associated with Tibetan Plateau forcing: I. Formation. *Climate Dynamics*, 39, 1169–1181. <https://doi.org/10.1007/s00382-012-1334-z>.
- Wu, G.X., Guan, Y., Liu, Y.M., Yan, J.H. and Mao, J.Y. (2012c) Air-sea interaction and formation of the Asian summer monsoon onset vortex over the Bay of Bengal. *Climate Dynamics*, 38, 261–279. <https://doi.org/10.1007/s00382-010-0978-9>.
- Wu, G.X., Duan, A.M., Liu, Y.M., Mao, J.Y., Ren, R.C., Bao, Q., He, B., Liu, B.Q. and Hu, W.T. (2014) Tibetan Plateau climate dynamics: recent research progress and outlook. *National Science Review*, 2, 100–116. <https://doi.org/10.1093/nsr/nwu045>.
- Wu, G.X., Zhuo, H.F., Wang, Z.Q. and Liu, Y.M. (2016) Two types of summertime heating over the Asian large-scale orography and excitation of potential-vorticity forcing I. Over Tibetan Plateau. *Science China Earth Sciences*, 59, 1996–2008. <https://doi.org/10.1007/s11430-016-5328-2>.
- Yanai, M., Li, C.F. and Song, Z.S. (1992) Seasonal heating of the Tibetan Plateau and its effects on the evolution of the Asian summer monsoon. *Journal of the Meteorological Society of Japan*, 70, 319–351. [https://doi.org/10.2151/jmsj1965.70.1B\\_319](https://doi.org/10.2151/jmsj1965.70.1B_319).
- Yang, K., Guo, X.F., He, J., Qin, J. and Koike, T. (2011) On the climatology and trend of the atmospheric heat source over the Tibetan Plateau: an experiments-supported revisit. *Journal of Climate*, 24, 1525–1541. <https://doi.org/10.1175/2010JCLI3848.1>.
- Yao, T.D., Thompson, L., Yang, W., Yu, W.S., Gao, Y., Guo, X.J., Yang, X.X., Duan, K.Q., Zhao, H.B., Xu, B.Q., Pu, J.C., Lu, A.X., Xiang, Y., Kattel, D.B. and Joswiak, D. (2012) Different glacier status with atmospheric circulations in Tibetan Plateau and surroundings. *Nature Climate Change*, 2, 663–667. <https://doi.org/10.1038/nclimate1580>.
- Ye, D.Z. and Wu, G.X. (1998) The role of the heat source of the Tibetan Plateau in the general circulation. *Meteorology and Atmospheric Physics*, 67, 181–198. <https://doi.org/10.1007/BF01277509>.
- Yeh, T.C., Lo, S.W. and Chu, P.C. (1957) The wind structure and heat balance in the lower troposphere over Tibetan Plateau and its surrounding. *Acta Meteorologica Sinica*, 28, 108–121. <https://doi.org/10.11676/qxxb1957.010> (in Chinese with English abstract).
- Yeh, T.C. and Gao, Y.X. (1979) *Qinghai-Xizang Plateau Meteorology*. Beijing: Science Press, pp. 1–278 (in Chinese).
- Zhang, S.L. and Tao, S.Y. (2001) Influences of snow cover over the Tibetan Plateau on Asian summer monsoon. *Chinese Journal of Atmospheric Sciences*, 25, 372–390 (in Chinese).
- Zhu, L.H., Huang, G., Fan, G.Z., Qu, X., Zhao, G.J. and Hua, W. (2017) Evolution of surface sensible heat over the Tibetan Plateau under the recent global warming hiatus. *Advances in Atmospheric Sciences*, 34, 1249–1262. <https://doi.org/10.1007/s00376-017-6298-9>.
- Zhu, L.H., Huang, G., Fan, G.Z., Qu, X., Wang, Z.B. and Hua, W. (2019) Elevation-dependent sensible heat flux trend over the Tibetan Plateau and its possible causes. *Climate Dynamics*, 52 (7–8), 3997–4009.

**How to cite this article:** Zhu L, Huang G, Fan G, et al. Evaluation of the dependence of the sensible heat flux trend on elevation over the Tibetan Plateau in CMIP5 models. *Int J Climatol*. 2021;41 (Suppl. 1):E3101–E3121. <https://doi.org/10.1002/joc.6908>